Title
18F-FDG PET/CT to measure glucose metabolism of various breast cancer cell lines in vivo

Author
Agrawal, Madhav

Publication Date
2013

Peer reviewed|Thesis/dissertation

18F-FDG PET/CT to measure glucose metabolism of various breast cancer cell lines *in vivo*

by

Madhav Agrawal

THESIS

Submitted in partial satisfaction of the requirements for the degree of

MASTER OF SCIENCE

in

Biomedical Imaging

in the

GRADUATE DIVISION

of the

UNIVERSITY OF CALIFORNIA, SAN FRANCISCO

Acknowledgement

I want to thank my PI, Dr. Youngho Seo for his guidance and support for this project. I also want to Dr. Luika Timmerman (Principle Investigator of this project) for her enthusiasm and support for understanding this project. I thank Dr. Henry Van Brocklin and Dr. Byron Hann for their supporting guidance on this project.

I want to thank Melanie Reagan and Stephanie Taylor Murphy for their support with the methods of this project.

I also want to thank my family and friends for their support.

Most importantly, I want to dedicate this paper to all the women who are susceptible to breast cancer.

^{18}FDG PET/CT to measure glucose metabolism of various breast cancer cell lines in vivo

Madhav Agrawal

Abstract

Introduction: Breast cancer is prevalent health issue in women. Currently PET scanning is used as a noninvasive means to provide physiological information the uptake of glucose and its metabolism. This is performed by using the ^{18}F-FDG tracer, which is a glucose analog. Currently, *in vitro* experiments are executed to understand the metabolism and glucose uptake of breast cancer cell lines in order to develop novel therapeutics. However, the *in* vitro glucose uptake data on breast cancer cell lines contradicts our speculation of how the trend should look, which is based off our understanding of cell line's characteristics in human models. The aim of our study is to ensure if glucose uptake *in vitro* correlates with *in vivo* glucose uptake (FDG tracer).

Methods: 7 breast cancer cell lines were bilaterally implanted with the same cell line in the mammary fat pad of immunodeficient mice (SCID and NSG). The mice were monitored for volume growth and were imaged by microPET/CT when the tumors reached about 200 mm^3. The mice were injected with about 200 μCi/0.1 ml concentrations.

Results and Discussions: Small correlation (R^2 = 0.08394) was between the comparisons of glucose uptake *in vitro* and FDG uptake *in vivo*. Imaging was seen as inconsistent for two different cell lines. No correlation (R^2 = 0.00666) was observed

in the comparison between volume (in all instance) and their corresponding FDG uptake. Volume growth was an issue with all the animals and it is speculated that the implantation procedure is not optimal. Low correlation (R^2 = 0.0352) is observed in the overall comparison between FDG uptakes and volume growth rate. A comparison was done to clarify if $\%ID/g_{max}$ can be used instead of SUV_{max}, which resulted in a strong correlation (as expected). Further studies are needed due to small sample size

Conclusion: At the end of the study, it was observed that glucose uptake *in vitro* does not correlate with FDG uptake *in vivo*. This has a strong implication that *in vitro* studies for glucose uptake might not be translated to *in vivo* uptake.

TABLE OF CONTENTS

LIST OF FIGURES

Introduction

Breast cancer is a leading problem in women because of its high incidence and mortality rate. In order to diagnose this illness, many methods including positron emission tomography (PET) are used. PET is a non-invasive technique that provides physiological information on the uptake of glucose and its metabolism. This utilizes a radiotracer known as ^{18}F-fluorodeoxyglucose (^{18}FDG) that emits positrons. FDG is a glucose analog that is taken up by glucose transporters and is trapped within the cell. Tumors need glucose at a much higher rate than surrounding nonproliferating tissues, in order to meet energy needs for anabolic substrates and ATP. Thus, FDG-PET allows visualization of the tumors and differentiates between regular nonproliferating tissues. FDG-PET tracer is commonly used for oncologic imaging since it provides an assessment of the tumor size, location, and response to treatments, through monitoring glucose uptake by tumors [1].

FDG-PET is the main imaging modality used to assess metastasis of most tumors except few such as prostate cancer. FDG uptake is generally avid in breast tumors. However, FDG-PET is not good at imaging some breast tumors such as invasive lobular carcinomas (tumor affecting lobules), small or noninvasive tumors, or tumors of lower glucose metabolism [1-3]. Nonetheless, there are several studies that show contradictory correlations between FDG visibility of breast tumors and their molecular or histological subtypes. This may be due to a low sample size, using different instruments or calculations for determining the signal intensity, or because of the differences in tumor sizes and stages [1, 4,5, 6-10].

Breast cancers can be classified by different criteria, and this impacts treatment response and prognosis. They are categorized by histopathological type, grade, stage (TNM), hormone receptor status, expression of the Her2 receptor tyrosine kinase, presence or absence of genetic mutations as determined by DNA testing, and comprehensive analysis of gene expression profiles. Histopathology is the microscopic examination of tissue to study manifestation of disease [11].

Grading is based on the microscopic similarity of breast cancer cells to normal breast tissues, and classifies the cancer as well differentiated (low grade), moderately differentiated (intermediate grade), and poorly differentiated (high grade). Less normal appearing cells (high grade) have worse prognosis than more normal appearing cells (low grade). The more similar the cancer cells look compared to normal cells, the slower their proliferation and better the prognosis. If cells are not well differentiated, they look immature, have active proliferation, and will likely metastasize [11].

Staging breast cancer using the TMN classification is based on the size of the tumor in its original location (T), and the location and size of tumor cells found in either regional lymph nodes (N), or in distal metastatic sites (M). Nucleic acid-based classification is based on assessment of specific DNA mutations or comprehensive gene expression profiles [11].

Receptor status of breast cancers is determined by immunohistochemistry (IHC), a process using antibodies or antisera to identify specific proteins expressed by tumor cells, usually using thin sections of formalin-fixed, paraffin embedded tumor. Breast tumor sections are routinely stained for expression of the estrogen

receptors (ER), progesterone receptors (PR), and Human Epidermal Growth Factor Receptor 2 (HER2). Her2 status is also determined by analysis of gene amplification at the HER2 locus. This is a common way of testing for receptor status; however, DNA multi-gene expression can arrange breast cancer into molecular subtypes, which bears approximate correspondence to IHC receptor status [11].

Receptor status is an important assessment for all breast cancer because these receptors have been shown to drive tumor proliferation, and effective, receptor-specific inhibitors exist which impede cell growth in both the adjuvant and neoadjuvent settings. For example, many estrogen receptor positive (ER+) tumors, which have better prognosis, depend on estrogen for their growth. They can be treated by drugs that block estrogen receptor activation, or drugs that lower the body's ability to synthesize estrogen [12]. HER+ tumors used to have poor prognosis, but drugs such as a monoclonal antibody that interacts with the receptor alongside with chemotherapy, has greatly improved the prognosis [12-13]. In contrast, triple negative (TNBC) cancer does not express receptors targeted by clinically available specific inhibitors (ER-, PR-, HER2-), and have comparatively poor prognosis [14-15].

Immunohistochemistry is the most common method for testing receptor status, though; DNA multi-gene expression profiles can categorize breast cancers into molecular subtypes, which also correspond to IHC receptor status. These molecular classes have different prognoses and may have different responses to specific therapies [11-16].

Molecular classes include:

- Basal-like: triple negative breast cancer (ER-, PR-, HER2-) [17].
- Luminal A: ER + with low grade
- Luminal B: ER+ with usually high grade
- ERBB2/HER2+: amplified HER2/neu [12]
- Claudin-low: usually triple-negative with low expression of cell-cell junction proteins and high frequency of lymphocyte infiltration [11,17-19].

There are currently several studies that analyzed the correlations between FDG-PET visibility of breast tumors and their molecular or histological subtype [1,4,5,6-10]. The results are contradictory, which may be because of the small study sizes, using different instruments or calculations for determining signal level, and the differences between tumor stages and sizes. There are several studies that conclude that triple negative human breast tumors (ER-, PR-, HER2-) show higher signal intensity with FDG-PET than in ER+ tumors (usually luminal A), based from clinical FDG-PET analysis of tumors in situ [6-9]. Moreover, there is one other study that demonstrates basal molecular subtypes to be better visualized than combined molecular subtypes [10]. Additional studies are need for comparing specific molecular subtypes, such as claudin low and luminal B tumors [20].

Dr. Luika Timmerman (Principal Investigator of this project) is a USCF researcher whose goal is to develop novel therapeutics that target unusual metabolic activity in breast cancer. She has worked with a panel of about 50 breast cancer-derived cell lines, which include several independent isolates of major breast cancer subtypes and breast oncogenes in their naturally occurring genetic contexts

[21]. In order to determine the breast cancers' metabolic activities, she measured glucose uptake rates *in vitro* and compared this within the several proliferating but non-tumorigenic epithelial cell derivatives.

This resulted in wide variation in glucose consumption among the breast cancer samples. There were particularly low glucose consumption rates in some basal and all claudin low cell lines. These results were unexpected because basal and claudin low cell lines are from tumors of poor prognosis with aggressive behavior. In comparison to her luminal-B tumor derivatives, they proliferate more rapidly and they aggressively spread in cultures on plastic or within extracellular matrix preparations [22, 23]. Because therapeutic development is intensively reliant on *in vitro* cell culture studies, we want to determine whether *in vitro* uptake values correspond with *in vivo* values. Substantial variation in glycolytic rate between these two different environments would suggest that the development of therapeutics that impede glycolysis might be better performed *in vivo*, and rely little if at all on studies performed *in vitro*. [20].

In collaborating with Dr. Timmerman in this study, we investigated our hypothesis: Glucose uptake rates that have been measured in breast cancer cell lines *in vitro* will correspond to the activity concentration of FDG in xenograft tumors *in vivo*. If this is true, then human breast tumors of specific molecular subtypes, such as claudin low tumors, might have faint FDG-PET signals *in situ* during clinical scans, and small metastases might be missed. This is important given that this subtype is proposed that these tumors are derived from stem cells [24, 25]. Similarly, bona

fide tumor stem cells might not be visualized, and a patient erroneously declared tumor free.

Although Dr. Timmerman's primary interest is in claudin low (ie. MDA-MB-231), high glucose avidity (MDA-MB-453) *in vitro* were included in order to see if *in vivo* glucose uptake corresponds with *in vitro* glucose uptake. The high glucose avidity breast cancer cells also serves to act as a control to prevent the slight possibility of having an unpredicted, confounding incompatibility between FDG-PET analysis and xenografted human breast cancer in mice [20].

Materials and Methods

Preparation of Breast Cancer Cells Xenografts:

The Preclinical Therapeutics Core at UCSF established xenografts with Dr. Timmerman's breast cell lines in 6-week old severe combined immunodeficiency (SCID) and NSG (NOD.Cg-Prkdc^{scid} Il2rg^{tm1Wjl}/SzJ) female mice. 7 breast cancer cell lines (had PET scans) out of 10 were used in this study to understand the *in vivo* FDG-PET uptake, ranging from very high to low *in vitro* glucose uptake[20]. The 7 cell lines included were BT474, HCC1954, MDA-MB-231, MDA-MB-415, MDA-MB-435, MDA-MB-436, and MDA-MB-453. The three cell lines not included in the study were HCC1569, HCC2185, and SUM52PE because of lack of tumor growth of mice tumors and/or death of the mice before scan.

Cell lines were implanted bilaterally into anesthetized mice with Matrigel carrier (BD Biosciences, San Jose, CA) in mammary fat pad 4 using 10^6-10^7 cells per injection [20].

FDG-PET analysis:

After the mice had been successfully implanted with the tumors, the mice were transferred to the Preclinical microPET/CT Imaging Core at UCSF (located in China Basin campus). This core monitored the mice 2-3 times per week, noting their tumor sizes, body weight, and general health as assessed by activity, coat appearance and behavior.

To allow for easy measurements, the mice were put under isoflurane anesthesia on top of a heat pad running at 30°C, tumor sizes measured using calipers, and tumor volumes calculated by standard methods. Once the tumors had reached a volume of 200 mm^3, the mice were prepared for imaging FDG-PET. In order to do this, the mice were fasted around 5pm the day before. The next day, about 200 μCi/ 0.1 ml concentration of FDG was intravenously injected (tail vein injection) after the mouse has been put under isoflurane anesthesia. PET scans were performed 55 minutes post injection, followed by a 10-minute static PET scan using a microPET/CT (dedicated PET combined with computed tomography, Inveon, Siemens Molecular Solutions, Malvern, PA) imaging modality. The CT portion of the scanner adds precision of anatomic localization to the PET functional imaging [20].

Image Reconstruction

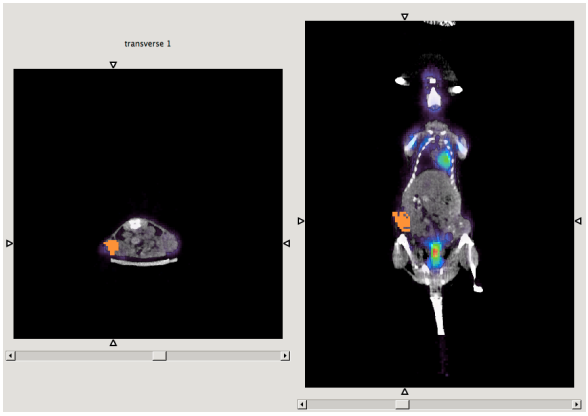

Figure 1: Xenograft imaging of the claudin low cell Line M435 using AMIDE and designating an ROI in the tumor where there is apparent FDG uptake.

After the scans were performed, the images were reconstructed and analyzed using the AMIDE imaging processing software. Metastasies were sought by visualizing increased signal throughout the body excluding the mammary fat pad, heart, and bladder. The areas where signal showed up, region of interests (ROIs) were drawn to figure out the amount of FDG-PET uptake. This was performed by calculating percentage of injected dose per gram [%ID/g] in tumors as shown in Figure 1. The maximum %ID/g values were used in order to avoid partial volume effect [20].

Dissection of Mice

Subsequent to imaging, Dr. Timmerman extracted the tumors and other tissues that had significant FDG-PET reactivity, also noting the appearance of the mouse, the gross structural details of the tumors and noting any visible abnormalities of internal anatomy. For example, we looked for tumor firmness and visible signs of tumor necrosis. At least half of all tumors were formalin fixed, for paraffin embedding and future histochemical and immunohistochemical analyses of

tumor morphology and expression of various specific molecules [20]. In some cases, parts of tumors and tissues were either embedded directly in OCT without fixation and frozen at -80°C for future production of frozen sections, and or directly flash frozen for future RNA extraction and analysis.

Results and Discussion

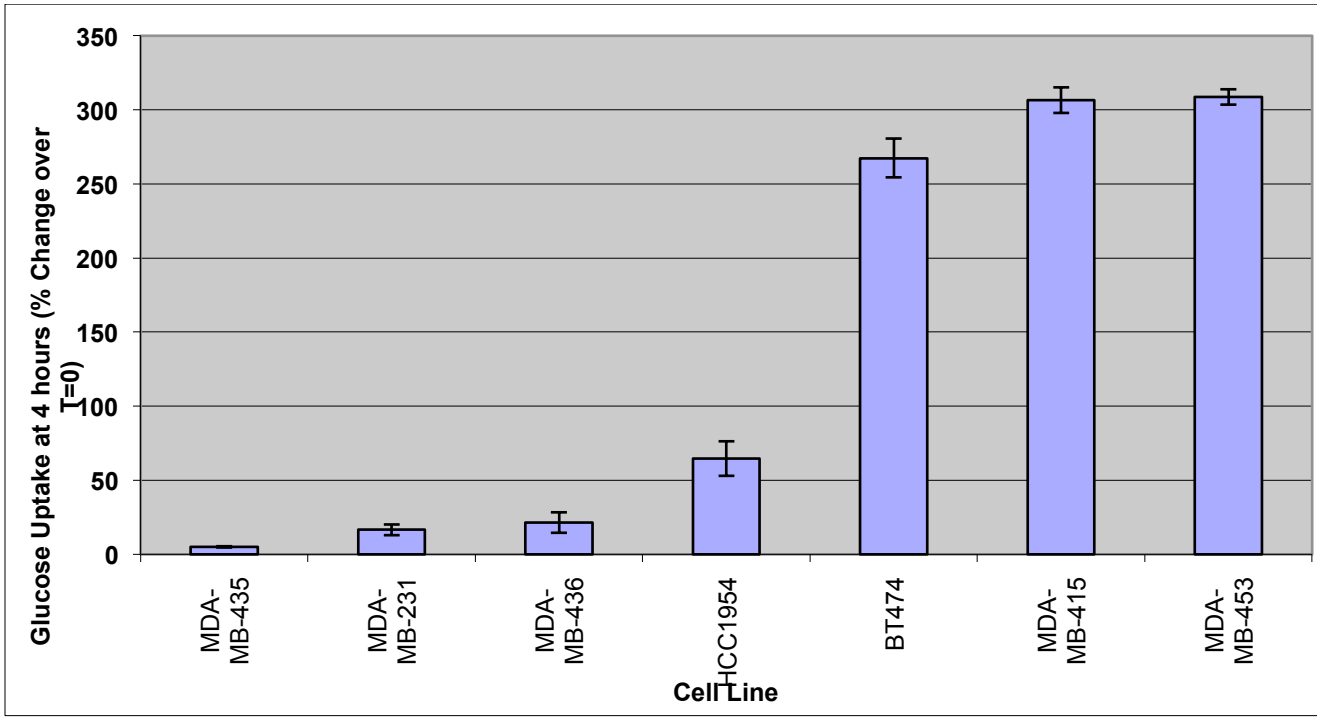

Figure 2: Relative *in vitro* glucose consumption of 7 human breast tumor-derived cell lines at 4 hours exposure to 2-NBDG or 6-NBDG fluorescent glucose (30μM, Molecular Probes N13195, N23106) [courtesy of Dr. Timmerman].

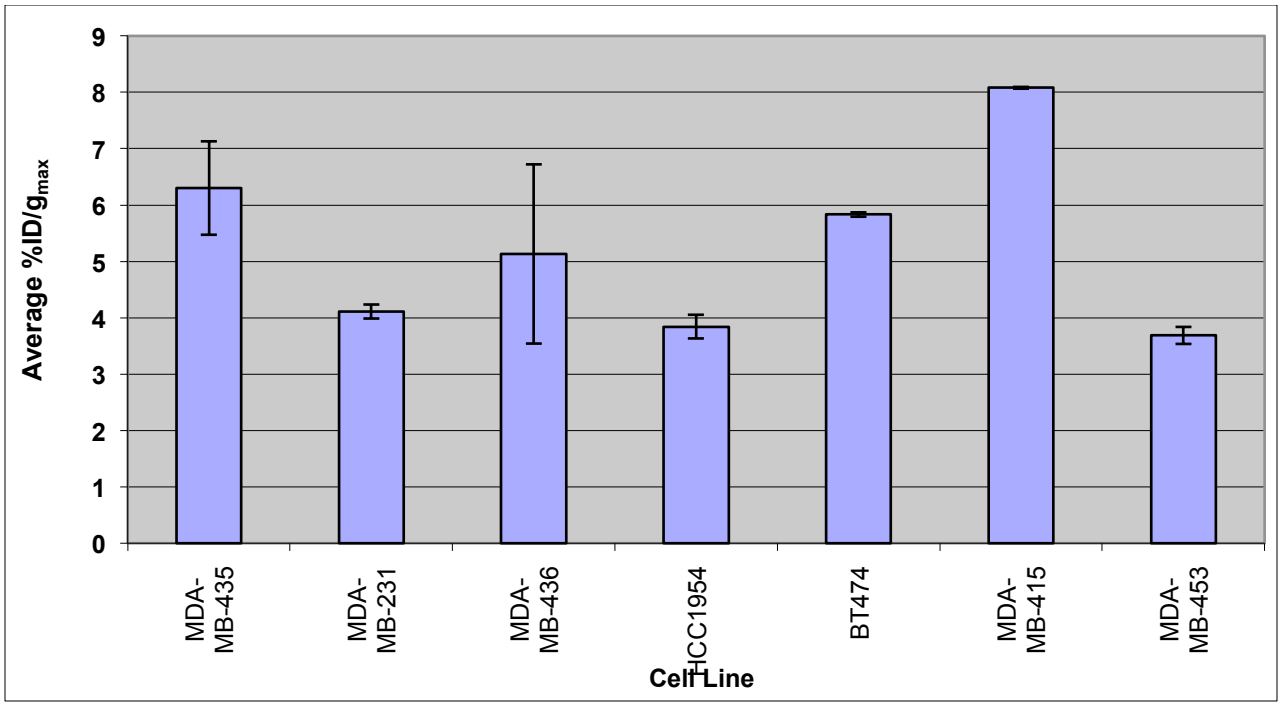

Figure 3: Relative average of FDG uptake in 7 xenograft cell lines [%ID/g_{max}] during FDG-PET scans.

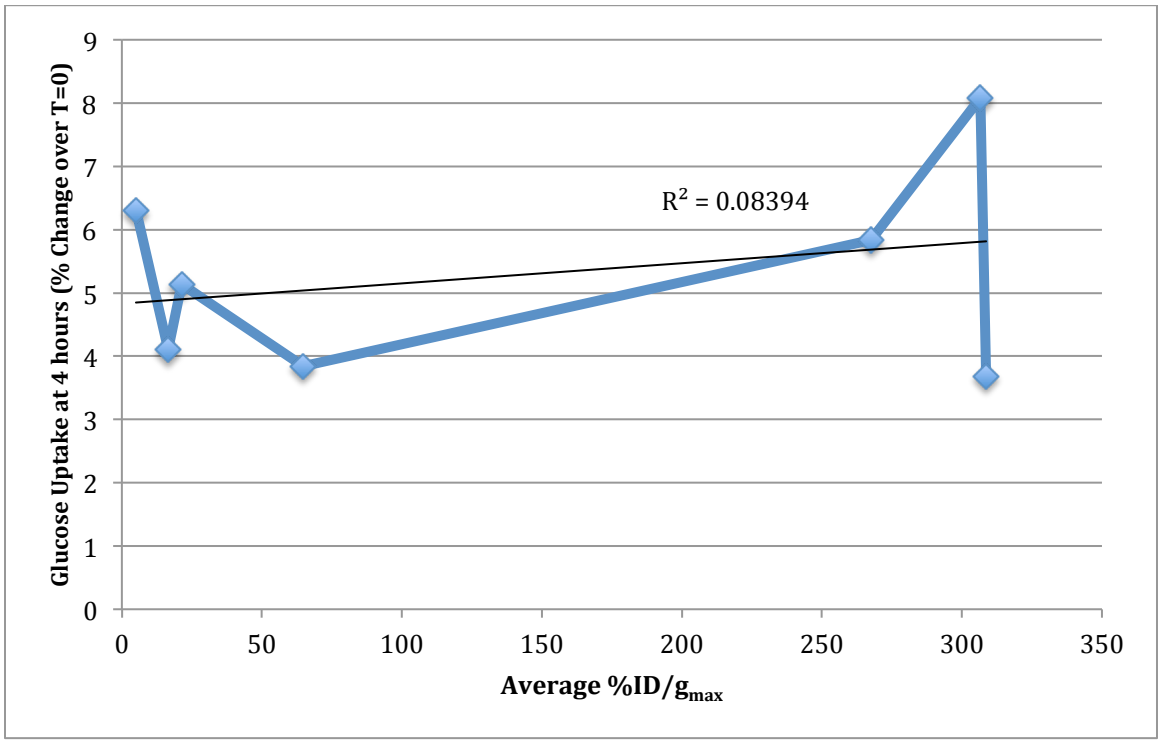

Figure 4: Comparison of glucose uptake *in vitro* (Figure 2) versus average FDG uptake *in vivo* (Figure 3) for 7 human breast cancer-derived cell lines.

Figure 2-4

Our studies revealed low correlation (R^2 = 0.08394) between *in vitro* glucose uptake and the *in vivo* FDG uptake values when comparing both the environmental situations [Figure 4]. This curve was generated from the average ID/g_{max} *in vivo* for the 7 breast cell lines included and comparing them with the corresponding glucose uptake *in vitro*.

The *in vitro* glucose uptake results were taken from Dr. Timmerman's preliminary study [Figure 2]. This entailed exposing subconfluent, exponentially growing cultures of various breast cancer-derived cell lines to a fluorescently labeled glucose molecule (2-NBDG or 6-NBDG glucose (30μM, Molecular Probes N13195, N23106)) for various times. Fluorescence of molecules adherent to the plasma membrane but not internalized was quenched by addition of Trypan Blue, and internalized fluorescence analyzed by Fluorescence Activated Cell Sorter (FACS). For each cell line, fluorescence intensity was normalized to that of parallel samples which were not exposed to labeled glucose. The 4 hour timepoint is used for these comparative studies with FDG-PET. This is standard protocol for doing immunohistochemical analysis *in vitro* [7]. The *in vivo* FDG-PET uptake [%ID/g] data [Figure 3] was determined from analysis of xenografts by micro PET/CT as described in the methods section of this thesis.

In Figure 3, it is seen that MDA-MB-435 has a high standard deviation, because of a difference in %ID/g in one MDA-MB-435 tumor from a mouse that was implanted bilaterally with two different tumors (MDA-MB-435 and MDA-MB 436].

We hypothesize that implantation of two different tumors may have produced crosstalk between these samples that altered their metabolic characteristics.

Interestingly, xenografts of MDA-MB436 have a high standard deviation because one of the scans had considerably high uptake for one tumor on the right and one considerably low uptake value on the left side [Figure 3]. It is unclear how that scan had two extremes; however, this directly demonstrates that non-genetic factors can play a strong role in glucose consumption rates of breast cancer xenografts. These factors may include such things as tumor size, vascularity, and or growth rates, and will be the subject of future analyses. More trivial but important technical reasons for these observed differences could be because of the amount of heat distributed in the mouse from the heat pad since isoflurane concentration and fasting time were standard and consistently implemented [26].

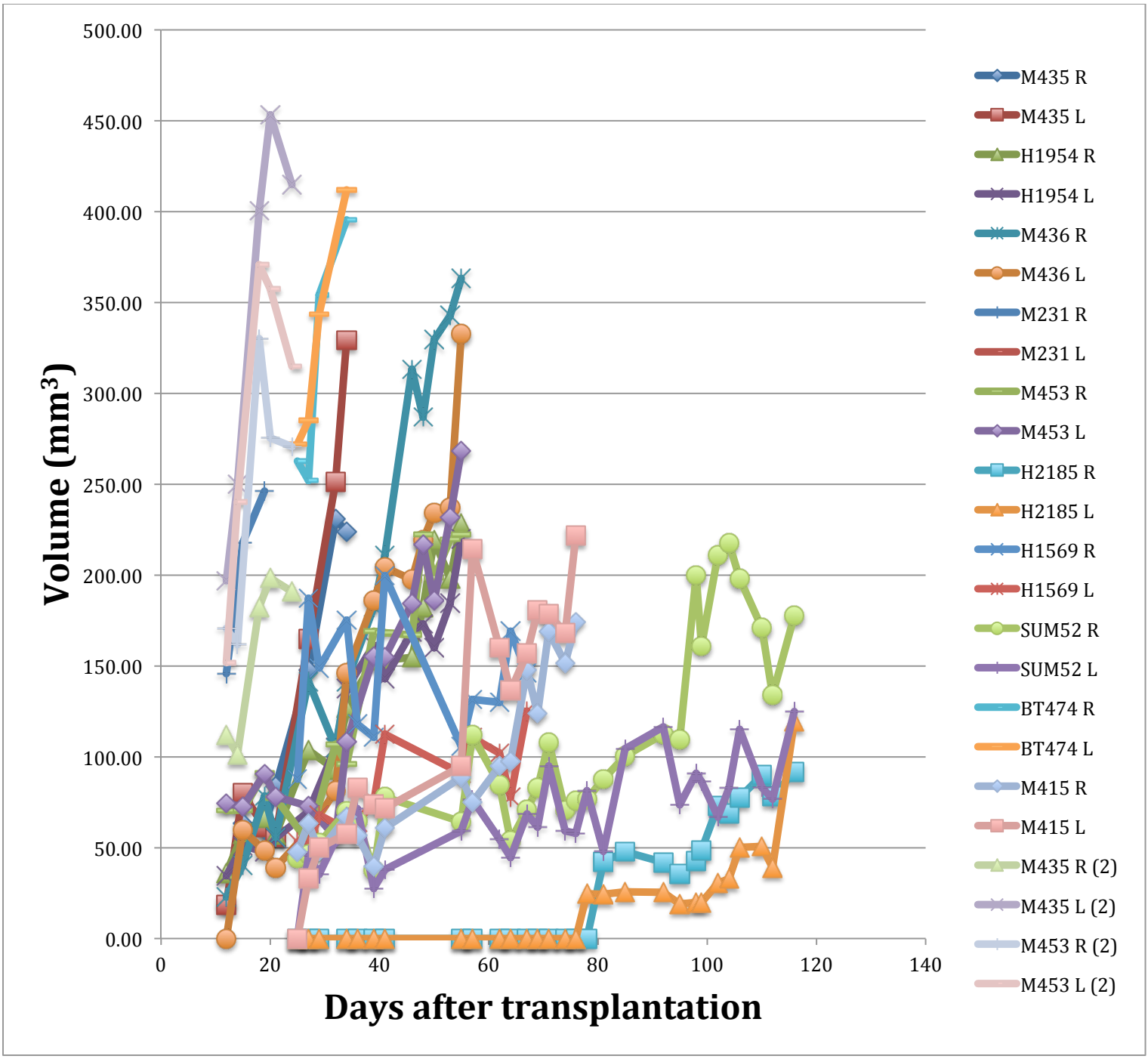

Figure 5: Growth curves of all xenografted cell lines (including the cell lines not included in FDG study). Growth of each tumor in bilateral implants was measured independently. This graph illustrates each individual animal their right (R) and left tumor (L).

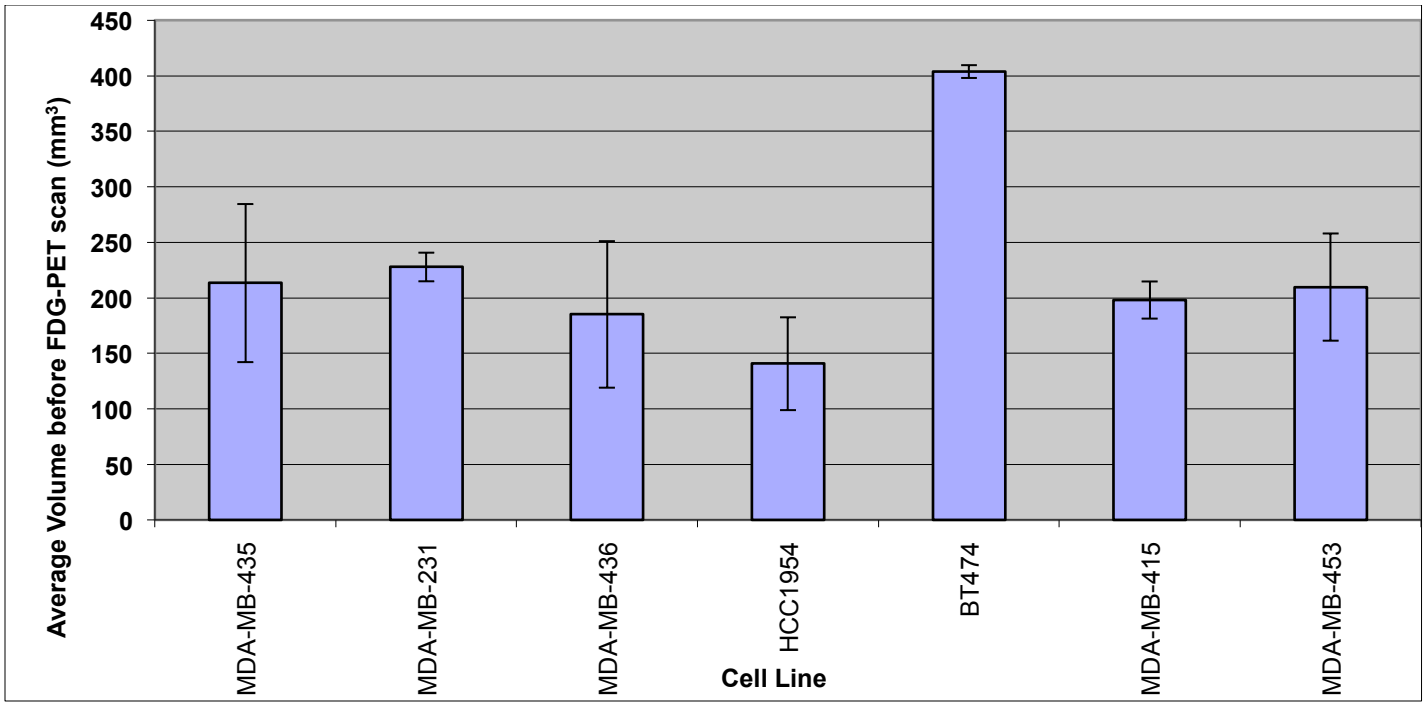

Figure 6: Comparison of average tumor volume for xenografts for each of the 7 breast cancer cell lines in the study.

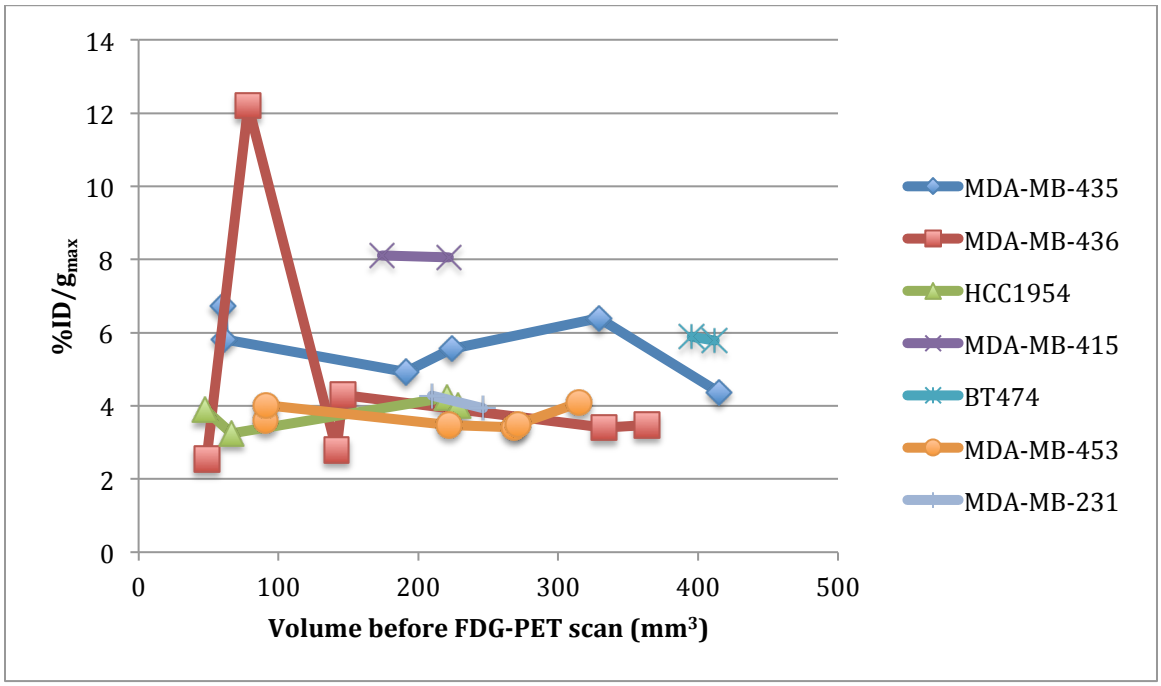

Figure 7: Comparison of FDG uptake *in vivo* versus tumor volume before FDG-PET-scan for each of the 7 breast cancer cell lines.

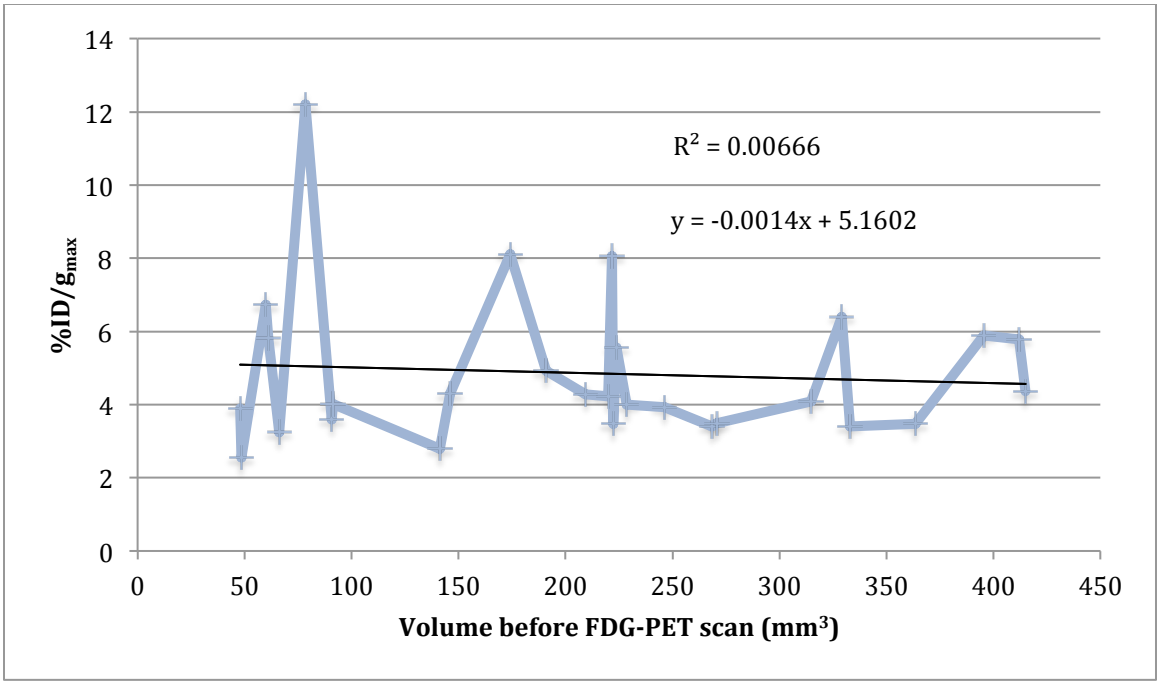

Figure 8: Comparison of overall volume (all instances) with their corresponding %ID/g_{max} for all 7 breast cancer cell lines.

Figure 5-8

Extremely low correlation (R^2 = 0.00666) is observed when comparing the volume determined before PET scan with FDG uptake values *in vivo*. These graphs were made by including each %ID/g_{max} value with its corresponding volume taken before the scan[Figure 7-8]. This data indicates that volume size does not account for the amount of FDG signal *in vivo*.

Tumor volume measurements were taken 2-3 times a week for each xenograft, individually recording the growth of left and right tumors [Figure 5]. The tumor sizes grew in a positive direction with some fluctuations [Figure 5]. The volumes had differing growth patterns and the sizes were variable between each cell line [Figure 6]. The xenografts of the luminal cell line HCC2185 grew poorly and stayed slightly palpable, which was why it was hard to measure the tumors. Since

the cell line's tumor did not grow to a minimum of 200 mm^3, the scans were not performed and therefore no uptake values are included. The xenografts of the luminal cell line SUM52PE also grew slowly, but eventually the tumors grew close to 200 mm^3. However, this cell line was also not included because the mouse had died before the scan.

We also observe the lack of growth in HCC2185 and slow growth of SUM52PE cell line (cell lines not included in study) may have been caused by human error in implanting the xenografts or an issue with Matrigel. Alternatively, many breast cancer-derived cell lines grow poorly in xenograft, with explanations that defy simple technical error. We chose to use fatpad implants of established cell lines, with Matrigel as a carrier, because this technique has been shown to be superior for establishment of many xenografts. We hypothesize that we might increase the odds of engraftment by injecting significantly more cells, changing the site of engraftment, or adding supporting human stroma such as fibroblasts to the injection mix. We will pursue these modifications in future studies. In HCC2185, the palpability of the tumors may have caused by the hardening of Matrigel, or by a fibrotic response of the host to the xenografted materials. Understanding the growth patterns of these xenografted breast tumors will help also help us understand whether the implantation protocol of the xenografts was optimal.

It is seen by the error bars that the tumor volume values of most of the cell lines have significant standard deviations, which further affects the correlation between uptake *in vivo* and volume of tumor [Figure 6]. This could have resulted from human error during the measurement process with the calipers.

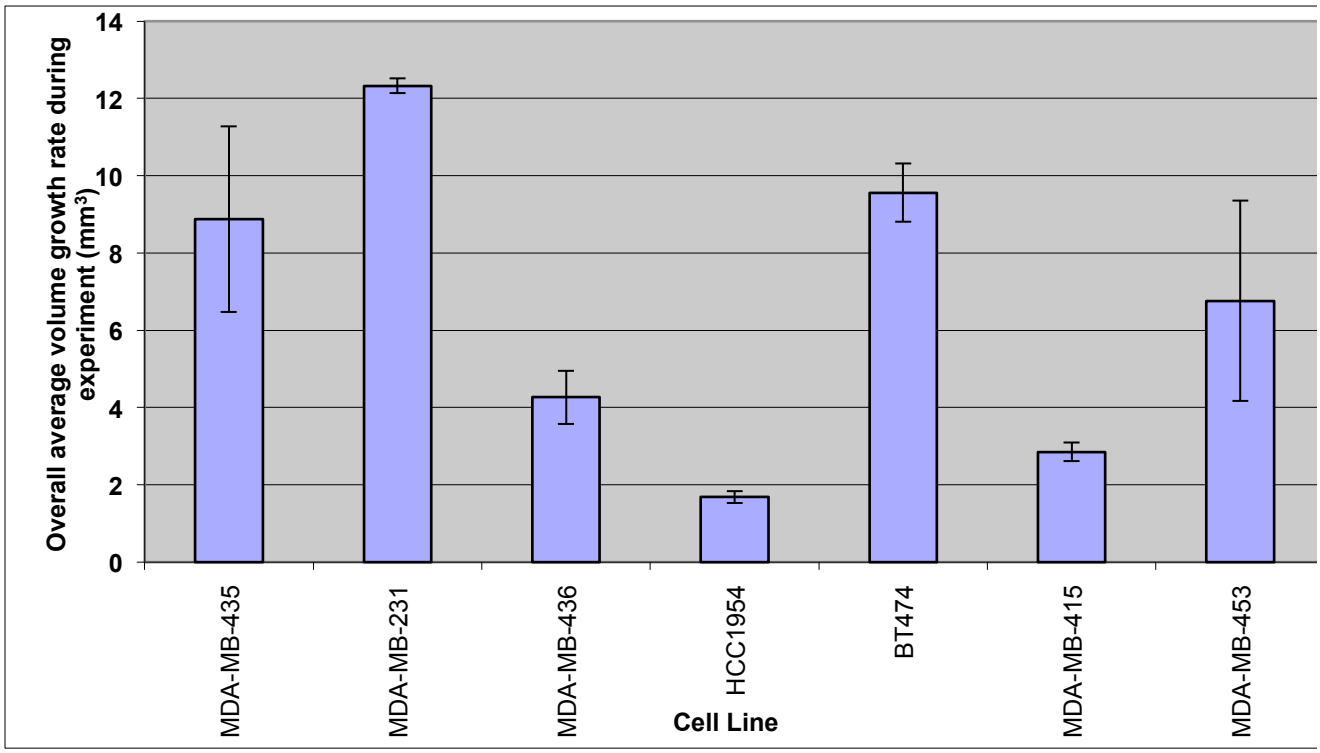

Figure 9: Comparison of overall average tumor growth rate during entire study for the 7 xenografted cell lines.

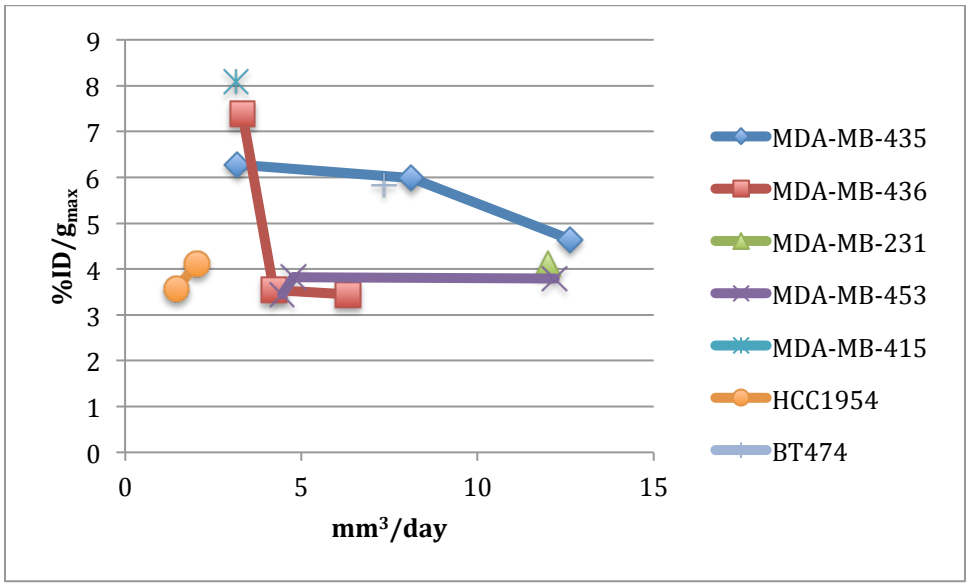

Figure 10: Comparison of FDG uptake *in vivo* versus volume growth per day based of imaging day for each of the 7 cell lines.

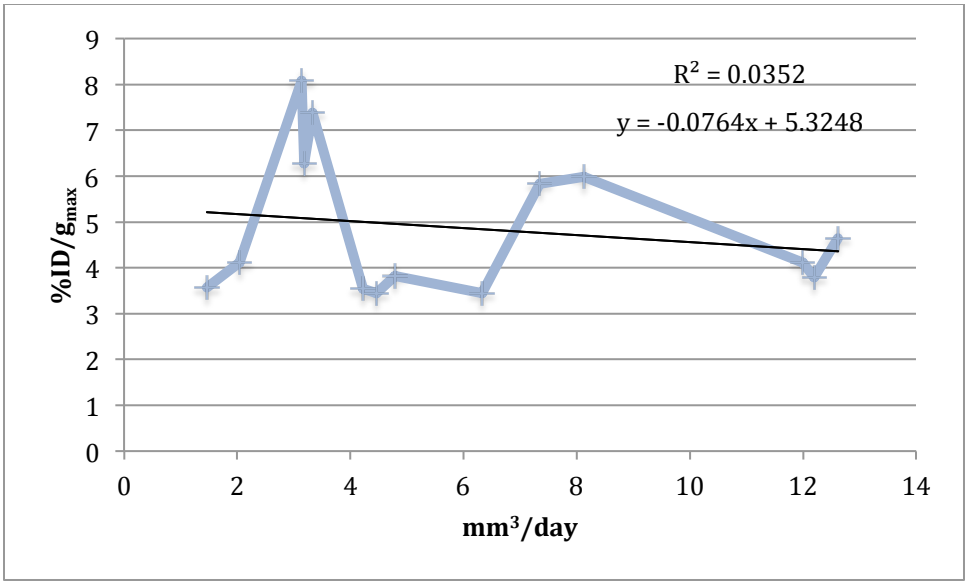

Figure 11: Overall comparison of FDG uptake *in vivo* versus volume growth per day based of imaging day for all the of the 7 cell lines.

Figure 9-11

Very low correlation is observed (R^2 = 0.0352) when comparing FDG-PET [%ID/g_{max}] *in vivo* with growth rate of tumors [mm^3/day] [Figure 10,11]. Therefore, the volume growth rate of tumors does not correlate with FDG uptake *in vivo*.

The volume growth rates are variable between each cell line measured [Figure 9]. The standard deviation for cell lines MDA-MB-435 and MDA-MB-453 are high. It is speculated that this error could have been because only those two cell lines each had two mice at different times during the course of the study.

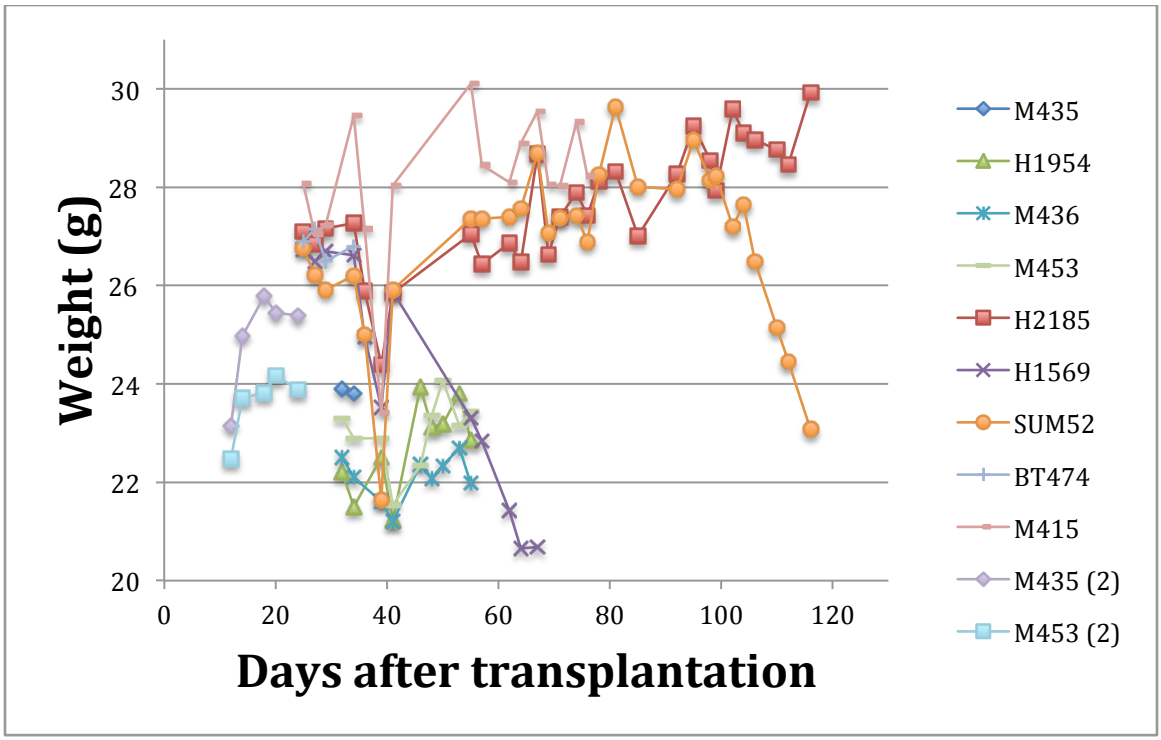

Figure 12: Mouse weights over the experimental time course. All xenografts were included, including the ones that were not scanned with PET. Xenograft with MDA-MB-231 not included.

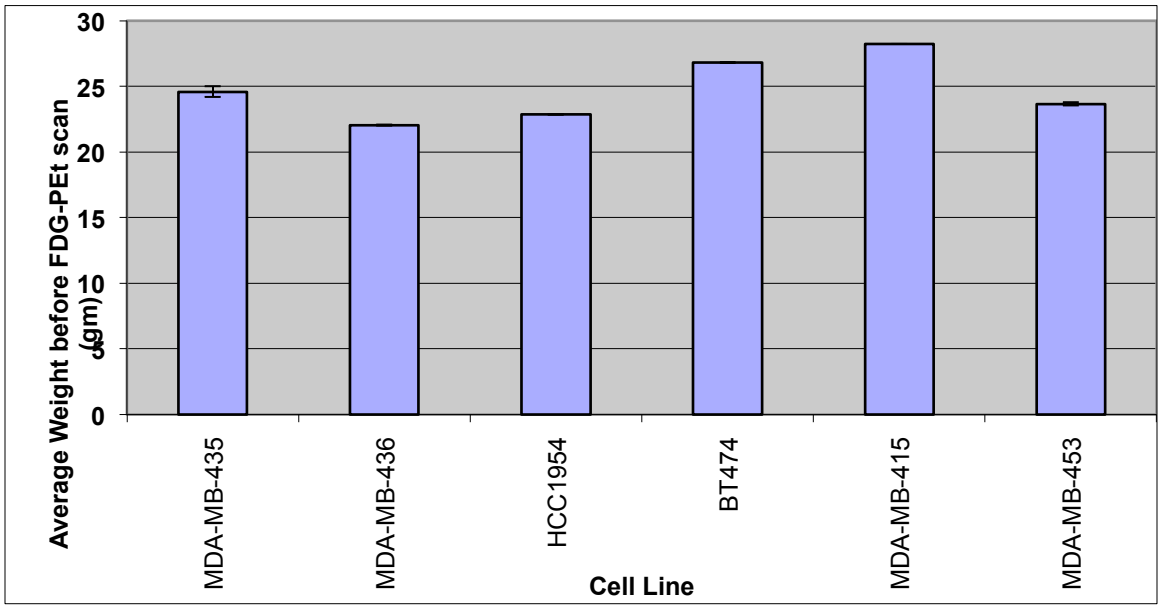

Figure 13: Comparison of average weight before FDG-PET scans for the 7 xenografted cell lines.

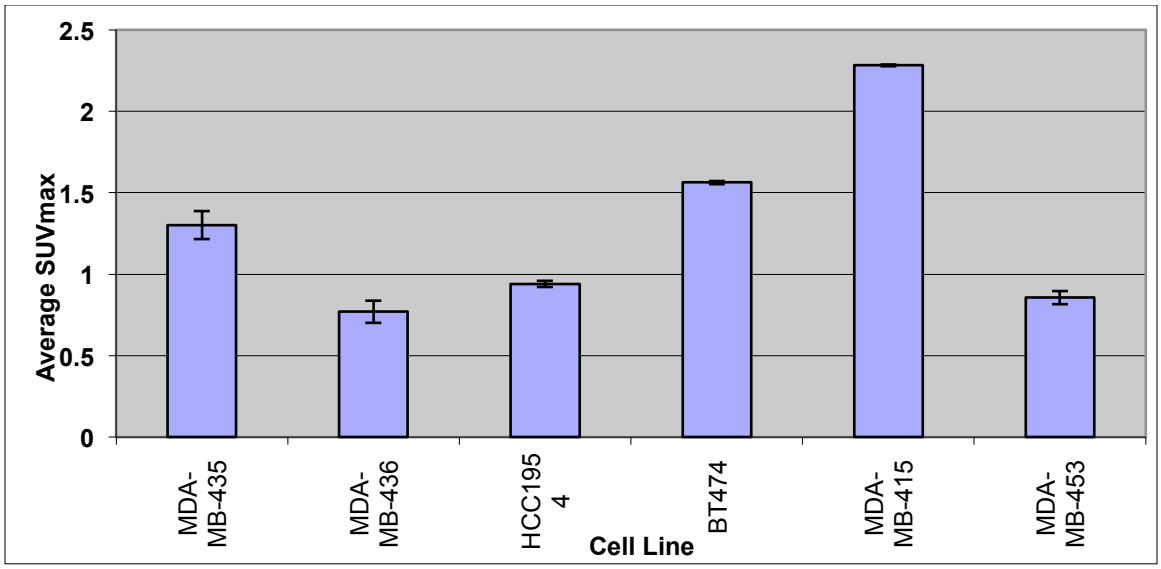

Figure 14: Comparison of average weight before FDG-PET scans for the 6 xenografted cell lines, which does not include MDA-MB-231.

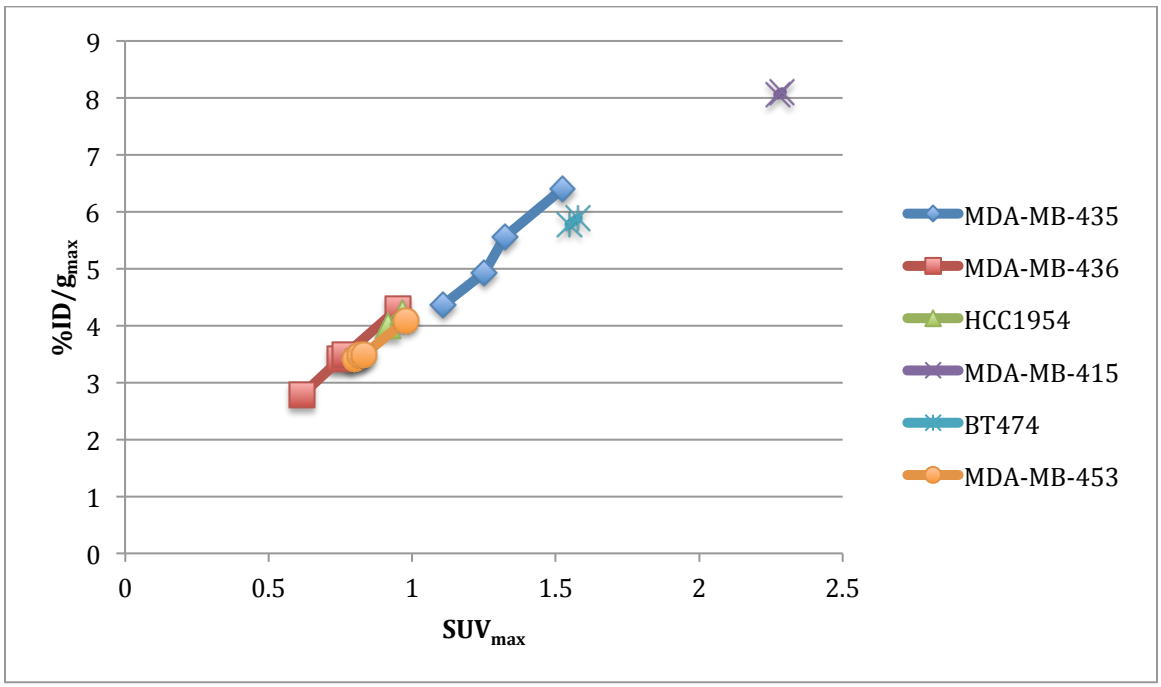

Figure 15: Comparison between average FDG uptake *in vivo* versus SUV_{max} (not inclusive of MDA-MB-231 xenograft).

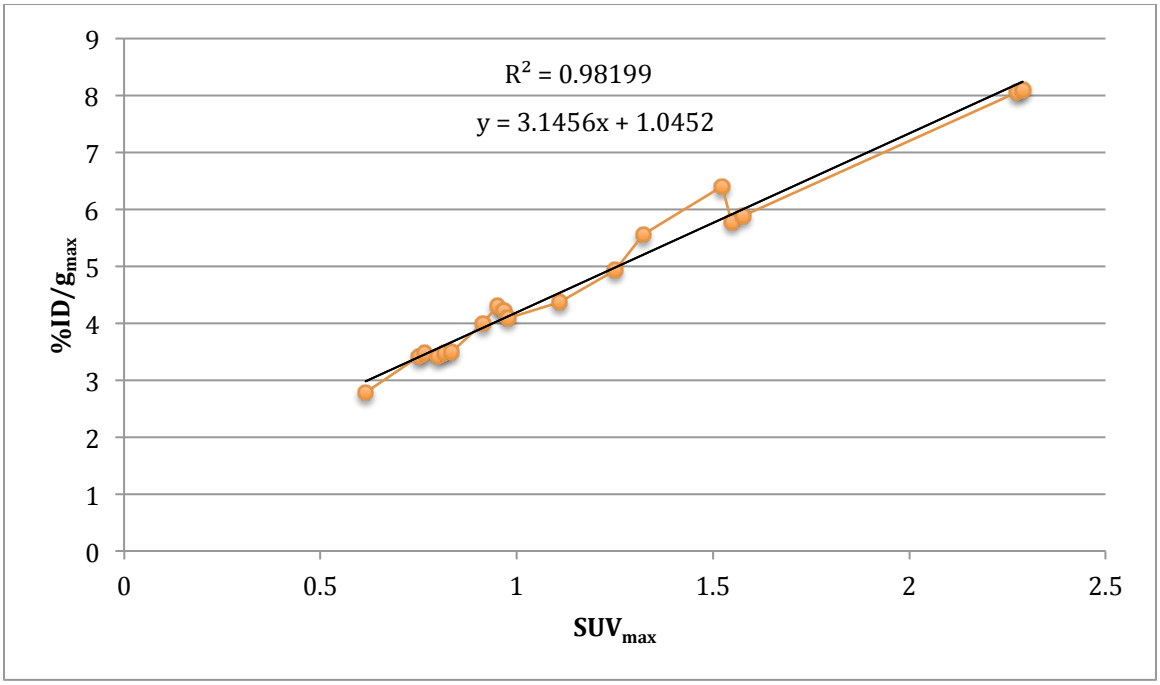

Figure 16: Overall comparison between average FDG uptake *in vivo* versus SUV_{max} (not inclusive of MDA-MB-231 xenograft).

Figure 12-16

While observing the overall comparison between the FDG uptakes *in vivo* versus SUV_{max}, the correlation was high ($R^2 = 0.98199$). Therefore, there is a strong positive linear relationship between SUV_{max} and $\%ID/g_{max}$ [Figure 16]

$\%ID/g_{max}$ was used instead of SUV_{max} because we did not feel the need to include the weight of the mice since the tumors were xenografted. But for reassurance, we included the weight of each animal to determine the SUV_{max}, which proved our assumption correctly.

Limitations and Future Studies

This study was on the level of a small project in order to allow us to understand how further studies need to be performed in order to solve our hypothesis: does *in vitro* glucose uptake correlate with *in vivo* glucose uptake.

But since this is a small project, there were a few limitations. The key issue was the amount of cell lines used in this study. We were only able to use 7 cell lines, but we would like to use about 50 breast cancer cell lines (Dr. Timmerman's panel). Also, we did not have the new *in vitro* glucose uptake values generated from the tumors used in this study. That would be a better way to see if there is any correlation between *in* vitro uptake of glucose compared to *in* vivo uptake of FDG-PET.

Another key issue is not having multiple scans on all the animals. Some had multiple scans while the tumors were growing to 200mm^3, but not for all, which may cause some discrepancies within the results since there were only few data points. Ideally, it would be better to have the entire cell lines implanted once and injected at the same time as other cell lines. Another thing would be to have all the scans done at the same time even if all animals have not reached 200 mm^3.

Further studies also need to be done in comparing the different implantation sites (ie. mammary fat pad, renal capsule, spine) and comparing different injection methods (ie. subcutaneous, intravenous injection, and intraperitoneal injection). Different types of tumors that are not breast cancers (ie. prostate cancer) also need to be analyzed to see if there is varying uptake between different cancer types. Most importantly other glucose analogs (ie. ^{11}C) also need to be used to see if there is a difference in signal uptake and to determine if FDG is an optimal tracer to view glucose uptake *in vivo*. Furthermore, looking at perfusion studies of uptake in these animals would be something of interest, which can be done by injecting ^{15}O [27].

This can provide uptake rates and distribution of injection *in vivo* to understand the characteristics FDG injection in the body.

Conclusions

In our measurements, the *in vitro* uptake of glucose versus *in vivo* uptake of FDG in breast tumors was not correlated. This has important implications that *in vitro* studies may not be useful in understanding glycolysis of tumors in vivo, and therapeutics designed to manipulate glycolytic events based in studies *in vitro*, may have little efficacy for tumors *in vivo*. However, since this is a small study in which the purpose is to give us better ideas in how to design future, comprehensive studies to answer the question if *in vitro* glucose uptake correspond to *in vivo* glucose uptake.

References:

1. Escalona, S., Blasco, J. A., Reza, M. M., Andradas, E., and Gomez, N. (2010). A systematic review of FDGPET in breast cancer. Med Oncol 27, 114-129.

2. Benard, F., and Turcotte, E. (2005). Imaging in breast cancer: Single-photon computed tomography and positron-emission tomography. Breast Cancer Res 7, 153-162.

3. Mavi, A., Urhan, M., Yu, J. Q., Zhuang, H., Houseni, M., Cermik, T. F., Thiruvenkatasamy, D., Czerniecki,
B., Schnall, M., and Alavi, A. (2006). Dual time point 18F-FDG PET imaging detects breast cancer with high sensitivity and correlates well with histologic subtypes. J Nucl Med 47, 1440-1446.

4. Avril, N., Menzel, M., Dose, J., Schelling, M., Weber, W., Janicke, F., Nathrath, W., and Schwaiger, M.
(2001). Glucose metabolism of breast cancer assessed by 18F-FDG PET: histologic and immunohistochemical tissue analysis. J Nucl Med 42, 9-16.

5. Crippa, F., Seregni, E., Agresti, R., Chiesa, C., Pascali, C., Bogni, A., Decise, D., De Sanctis, V., Greco, M., Daidone, M. G., and Bombardieri, E. (1998). Association between [18F]fluorodeoxyglucose uptake and postoperative histopathology, hormone receptor status, thymidine labelling index and p53 in primary breast cancer: a preliminary observation. Eur J Nucl Med 25, 1429-1434.

6. Mavi, A., Cermik, T. F., Urhan, M., Puskulcu, H., Basu, S., Yu, J. Q., Zhuang, H., Czerniecki, B., and Alavi, A. (2007). The effects of estrogen, progesterone, and C-erbB-2 receptor states on 18F-FDG uptake of primary breast cancer lesions. J Nucl Med 48, 1266-1272.

7. Osborne, J. R., Port, E., Gonen, M., Doane, A., Yeung, H., Gerald, W., Cook, J. B., and Larson, S. (2010). 18F-FDG PET of locally invasive breast cancer and association of estrogen receptor status with standardized uptake value: microarray and immunohistochemical analysis. J Nucl Med 51, 543-550.

8. Wang, C. L., MacDonald, L. R., Rogers, J. V., Aravkin, A., Haseley, D. R., and Beatty, J. D. (2011). Positron emission mammography: correlation of estrogen receptor, progesterone receptor, and human epidermal growth factor receptor 2 status and 18F-FDG. AJR Am J Roentgenol 197, W247-255.

9. Basu, S., Chen, W., Tchou, J., Mavi, A., Cermik, T., Czerniecki, B., Schnall, M., and Alavi, A. (2008). Comparison of triple-negative and estrogen receptor-positive/progesterone receptor-positive/HER2-negative breast carcinoma using quantitative fluorine-18 fluorodeoxyglucose/positron emission tomography imaging parameters: a potentially useful method for disease characterization.

Cancer 112, 995-1000.

10. Palaskas, N., Larson, S. M., Schultz, N., Komisopoulou, E., Wong, J., Rohle, D., Campos, C., Yannuzzi, N., Osborne, J. R., Linkov, I., et al. (2011). 18F-fluorodeoxy-glucose positron emission tomography marks MYC-overexpressing human basal-like breast cancers. Cancer Res 71, 5164-5174.

11. Prat, A.; Perou, C. M. (2011). "Deconstructing the molecular portraits of breast cancer". *Molecular Oncology* **5** (1): 5–23.

12. Molecular origin of cancer: gene-expression signatures in breast cancer, Christos Sotirou and Lajos Pusztai, N Engl J Med 360:790 (2009 Feb 19).

13. Romond EH, Perez EA, Bryant J, et al. Trastuzumab plus adjuvant chemotherapy for operable HER2+ breast cancer. N Engl J Med. 2005; 353:1673-1684

14. Dent R, Trudeau M, Pritchard KI, Hanna WM, Kahn HK *et al* (2007-08-01). "Triple-Negative Breast Cancer: Clinical Features and Patterns of recurrence". *Clinical Cancer Research* (American Association for Cancer Research) **13** (15 Pt 1): 4429–4434.

15. "Understanding and Treating Triple-Negative Breast Cancer". Cancer Network. Retrieved 2010-05-08.

16. Geyer, F. C.; Marchiò, C.; Reis-Filho, J. S. (2009). "The role of molecular analysis in breast cancer".*Pathology* **41** (1): 77–88.

17. Perou, C. M. (2011). "Molecular Stratification of Triple-Negative Breast Cancers". *The Oncologist* **16**: 61–70.

18. Herschkowitz, J. I.; Zhao, W.; Zhang, M.; Usary, J.; Murrow, G.; Edwards, D.; Knezevic, J.; Greene, S. B.; Darr, D.; Troester, M. A.; Hilsenbeck, S. G.; Medina, D.; Perou, C. M.; Rosen, J. M. (2011). "Breast Cancer Special Feature: Comparative oncogenomics identifies breast tumors enriched in functional tumor-initiating cells". *Proceedings of the National Academy of Sciences* **109** (8): 2778.

19. Harrell, J. C.; Prat, A.; Parker, J. S.; Fan, C.; He, X.; Carey, L.; Anders, C.; Ewend, M. et al. (2011)."Genomic analysis identifies unique signatures predictive of brain, lung, and liver relapse". *Breast Cancer Research and Treatment* **132** (2): 523–535.

20. Timmerman, L. Research Proposal. 2013.

21. Neve, R. M., Chin, K., Fridlyand, J., Yeh, J., Baehner, F. L., Fevr, T., Clark, L., Bayani, N., Coppe, J. P.,Tong, F., et al. (2006). A collection of breast cancer cell lines for the

study of functionally distinct cancer subtypes. Cancer Cell 10, 515-527.

22. Sommers, C. L., Byers, S. W., Thompson, E. W., Torri, J. A., and Gelmann, E. P. (1994). Differentiation state and invasiveness of human breast cancer cell lines. Breast Cancer Res Treat 31, 325-335.

23. Han, J., Chang, H., Giricz, O., Lee, G. Y., Baehner, F. L., Gray, J. W., Bissell, M. J., Kenny, P. A., and Parvin, B. (2010). Molecular predictors of 3D morphogenesis by breast cancer cell lines in 3D culture. PLoS Comput Biol 6, e1000684.

24. Hennessy, B. T., Gonzalez-Angulo, A. M., Stemke-Hale, K., Gilcrease, M. Z., Krishnamurthy, S., Lee, J. S., Fridlyand, J., Sahin, A., Agarwal, R., Joy, C., et al. (2009). Characterization of a naturally occurring breast cancer subset enriched in epithelial-to-mesenchymal transition and stem cell characteristics. Cancer Res 69, 4116-4124.

25. Prat, A., Parker, J. S., Karginova, O., Fan, C., Livasy, C., Herschkowitz, J. I., He, X., and Perou, C. M. (2010). Phenotypic and molecular characterization of the claudin-low intrinsic subtype of breast cancer. Breast Cancer Res 12, R68.

26. Fuerger, B. J., Czernin, J., Hilderbrandt, I., Tran, C., Hapern, B. S., Stout, D., Phelps, M.E., Wever, W. A. (2006). Impact of Animal Handling on the Results of ^{18}F-FDG PET Studies in Mice.

27. Haberkorn, U., Strauss, L. G., Resisser, Ch., Haag, D., Dimitrakopoulou, A., Ziegler, S., Oberdorfer, F., Rudat, V., van Kaick, G. (1991). Glucose Uptake, Perfusion, and Cell Prolifeartion in Head and Neck Tumors: Relation of Positron Emission Tomography to Flow Cytometry.

Publishing Agreement

It is the policy of the University to encourage the distribution of all theses, dissertations, and manuscripts copies of all UCSF theses, dissertations, and manuscripts will be routed to the library via the Graduate Division. The library will make all theses, dissertations, and manuscripts accessible to the public and will preserve these to the best of their ability, in perpetuity.

Please sign the following statement:

I hereby grant permission to the Graduate Division of the University of California, San Francisco to release copies of my thesis, dissertation, or manuscript to the Campus Library to provide access and preservation, in whole or in part, in perpetuity.

Author Signature

9/10/13

Date